OPEN ACCESS International Journal of Pharmacology

ISSN 1811-7775
DOI: 10.3923/ijp.2020.554.561

Research Article
Thymoquinone Loaded Zein Nanoparticles Improves the Cytotoxicity against Breast Cancer Cells

[1]Usama A. Fahmy, [1]Osama A.A. Ahmed, [2]Mohamed A. El-moselhy, [3]Hani Z. Asfour and [1,4,5]Nabil A. Alhakamy

[1]Department of Pharmaceutics, Faculty of Pharmacy, King Abdulaziz University, Jeddah 21589, Saudi Arabia
[2]Department of Pharmacology, School of Pharmacy, Ibn Sina National College for Medical Studies, Al Mahjar Street, Jeddah, 22421, Saudi Arabia
[3]Department of Microbiology and Pathology, Faculty of Medicine, King Abdulaziz University, Jeddah 21542, Saudi Arabia
[4]Center of Excellence for Drug Research and Pharmaceutical Industries, King Abdulaziz University, Jeddah 21589, Saudi Arabia
[5]Mohamed Saeed Tamer Chair for Pharmaceutical Industries, King Abdulaziz University, Jeddah 21589, Saudi Arabia

Abstract

Background and Objective: Thymoquinone (TQ) has been reported for its efficacy to inhibit various cancer stages. Nanoparticles (NPs), showed great promise as drug carriers for cytotoxic agents. This study aims to investigate the ability of zein based NPs to enhance TQ cytotoxicity in MCF-7 cells. **Materials and Methods:** TQ was loaded on ZN NPs using the antisolvent phase separation technique. The prepared TQ ZN NPs were investigated for size, shape, *in vitro* release and cytotoxicity activity in MCF-7 cells. The presentation of data was performed using mean±SD. The IBM Statistical Package for Social Science (SPSS) statistics software (version 25) (SPSS Inc., Chicago, IL, USA) was utilized for carrying out statistical analysis. **Results:** TQ-Zein NPs revealed spherical shaped NPs with *in vitro* TQ sustained release for over 36 hrs and enhanced cytotoxicity activity in MCF-7 cells when compared with either pure TQ or ZN. Cell cycle analysis results showed accumulation of MCF-7 cells in G2/M and pre-G1 phases were observed in MCF-7 cells challenged with TQ ZN NPs. A significant increase in the % of cells for early and late apoptosis in addition to the total cell death as shown by cells stained with annexin V. **Conclusion:** Formulation of TQ in the form of ZN based NPs improved cellular permeation and apoptotic activity of TQ that leads to potentiation of its cytotoxic activities against MCF-7cells.

Key words: Thymoquinone, formulations, breast cancer, apoptosis, nanoparticles, nutraceuticals, eco-friendly, micelles

Citation: Fahmy, U.A., O.A.A. Ahmed, M.A. El-moselhy, H.Z. Asfour and N.A. Alhakamy, 2020. Thymoquinone loaded zein nanoparticles improves the cytotoxicity against breast cancer cells. Int. J. Pharmacol., 16: 554-561.

Corresponding Author: Usama A. Fahmy, Department of Pharmaceutics, Faculty of Pharmacy, King Abdulaziz University, Jeddah 21542, Saudi Arabia

Competing Interest: The authors have declared that no competing interest exists.

Data Availability: All relevant data are within the paper and its supporting information files.

INTRODUCTION

Thymoquinone (TQ) is a monoterpene and the main active volatile oil ingredient of black cumin (black seed) *Nigella sativa* L. (NS) family Ranunculaceae. Black seed is used as herbal (natural) medicine and condiment[1,2]. NS oil is used for the treatment of various health problems as bronchial asthma, gastrointestinal problems, hypertension and obesity. Clinical investigations on black seed extract taken orally have shown promising antioxidant and anti-inflammatory effects[3,4]. Besides, the efficacy of NS extract has shown results of cancer prevention and treatment[5]. TQ as a volatile oil ingredient of NS has been reported in various studies to have pharmacological properties[6-9]. Among these studies, the anticancer effects of TQ with selective cytotoxicity for cancer cells[7,10-16]. Besides, TQ augments chemotherapy and radiotherapy treatments through the sensitization of cancer cells affecting the resistance mechanisms[17,18]. The promising data for TQ as an antitumor agent is hindered by the low bioavailability of TQ.

Zein (ZN) a protein from natural plant origin is approved by the FDA and is generally recognized as a safe excipient[19-21]. The hydrophobic properties of ZN, because of its high content of hydrophobic amino acids, allow its use as a moisture barrier in the food industry[22-28]. Besides, ZN has been reported in formulation studies to form colloidal aggregates in physiological conditions that allow its use as a matrix for nano/ micro-particles formation[26,29-31]. Reports have indicated liver targeting characteristics of ZN as a drug carrier[32,33]. ZN nanospheres have been studied for sustained drug delivery applications for small drug molecules and macromolecules for oral and parenteral routes[30,34-40]. ZN has shown antioxidant and cytotoxic activities[41,42]. This work aimed to formulate the TQ loaded ZN nanoparticles (NPs) to enhance TQ cytotoxic activity against breast cancer cells and evaluate the role of ZN as a drug carrier for TQ.

MATERIALS AND METHODS

Study area: This study was carried out at the Nanotechnology Lab and cell culture lab, Department of Pharmaceutics, King Abdulaziz University, Jeddah, Saudi Arabia and from June, 2019-August, 2020.

Drug and chemicals: The TQ, ZN and ethanol were all purchased from Sigma-Aldrich (St. Louis, MI, USA). Dulbecco's Modified Eagle Medium (DMEM), streptomycin, penicillin, Fetal Calf Serum (FCS), trypsin-EDTA (0.05%) and phosphate buffer (PBS pH 7.4) were purchased from Thermo Fisher Scientific Inc. (Waltham, MA, USA).

TQ-ZN NPs formulation: TQ-ZN NPs as previously reported was prepared with slight modification[32]. In short, TQ was dissolved in absolute ethanol and ZN was dissolved in 90% ethanol. Both alcoholic solutions were mixed and then added to an aqueous solution of PVA (1 % w/v) and stirred for 4 h and then subjected to evaporation of ethanol. The TQ-ZN NPs dispersion was separated by centrifugation at 20,000 rpm for 30 min at 8°C then washed with deionized water (two cycles), then lyophilized and stored until fully characterized.

TQ-ZN NPs size and zeta potential evaluation: A sample from the prepared TQ-ZN NPs was dispersed in deionized water and then analyzed for size and zeta potential using Zetasizer Nano ZSP (Malvern Panalytical, Malvern, UK). The average of five runs was used for the determination of TQ-ZN NPs size and zeta potential.

TQ-ZN NPs encapsulation efficiency: The prepared TQ-ZN NPs formula sample was dissolved in ethanol and then injected into high-performance liquid chromatography (HPLC) analysis was obtained by an Agilent 1100 liquid chromatography (Wilmington, DE, USA) that contained a micro vacuum degasser (model G1379A), quaternary pump (model G1311A), multiple wavelength detector (model G13658) and analyzed for TQ content as previously reported[43]. Equation 1[44] was used to determine the Encapsulation Efficiency (EE) percentage of TQ:

$$EE\ (\%) = \left(\frac{\text{Amount of TQ in the NP}}{\text{Amount of TQ initially added}}\right) \times 100$$

TQ-ZN NPs *in vitro* diffusion study: An automated vertical Franz diffusion cell (MicroettePlus, Hanson Research, Chatsworth, CA, USA) was used for the diffusion study as previously described[45]. A diffusion buffer (pH 7.0) containing Tween 20 (0.5% w/v) stirred at 400 rpm and a diffusion membrane (0.1 µm) were utilized. Samples were collected at specified time intervals. TQ content in the withdrawn aliquots was analyzed by HPLC as previously reported[46].

Scanning electron microscopy: The sample preparation for investigation was carried out after securing these metallic stubs by utilizing the sticky tape (double-sided). The sticky tape was then fused to aluminum stubs and the vacuum was utilized for performing gold coating. The scanning electron microscope, model JEM 100-CX, JEOL (Tokyo, Japan) was utilized for assuring the availability of the selected TQ-ZN formula's surface morphology for carrying out analysis.

Cells and culture of cells: The MCF-7 cells were procured from the Vacsera located in Giza, Egypt. The maintenance of cells was assured out by using Dulbecco's Modified Eagle Medium (DMEM). 100 units mL^{-1} of Penicillin, 100 µg mL^{-1} of streptomycin and 10% of heat-inactivated fetal bovine serum (10%) were utilized for supplementing the culture medium. Moreover, 37°C temperature and CO_2 humidified (v/v) atmosphere (5%) was considered for keeping the cells within the state of sub-confluence.

Anti-proliferative activity assessment: The assessment of the prepared plain formula of TQ and ZN and TQ-ZN NPs against the MCF-7 liver cancer cells was carried out by using Sulforhodamine B (SRB). Moreover, the assessment of considered preparations' anti-proliferative activities against the human esophageal epithelial cells (HEEpiC) was also carried out. The seeding of cells was carried out into 96 well plates having 1000-2000 cells per well and trypsinization was carried out by using 0.25% Trypsin-EDTA. The treatment of cells was carried out by using the serial concentrations of the isolated compounds for 72 hrs. Afterward, 10% of trichloroacetic acid (TCA) was utilized for fixing the cells for 1 h, at a temperature of 4°C. All cells were splashed multiple times with water, which was followed by the utilization of 0.4% SRB solution was f or staining of cells. This process was followed by keeping them in the dark at room temperature for 10 min. The washing of cells was carried out by using 1% glacial acetic acid. After which the plates were left for drying overnight and Tris-HCl was utilized for dissolving the SRB-stained cells. The determination of color intensity (OD) was carried out by using the monochromator SpectraMax® M3 plate reader (Molecular Devices, Sunnyvale, CA, USA) at 540 nm. OD measurements were then utilized for calculating the growth inhibition (IC_{50}) percentage. The measurement of concentration was carried out three times and the complete experiment was carried out three times.

Progression analysis of cell cycle: Approximately 3×105 cells per well into N = 6 well-culture plates were seeded. The controlled incubation was performed and the cells were treated within the drug-free media, which was followed by challenging the cells with TQ-ZN NPs (5.3 µg mL^{-1}) and equal concentrations of TQ and ZN for 24 hrs. The investigation of the cell cycle was performed by using CycleTEST™ PLUS DNA Reagent Kit (Becton Dickinson Immunocytometry Systems, San Jose, CA, USA). Those cells which have a known DNA content (PBMCs) were considered as a control for test samples' DI (DNA index). According to instructions provided by the manufacturers, the staining process was performed by using Propidium iodide. Moreover, for carrying out cell cycle distribution analysis, the DNA cytometer and CELLQUEST software (Becton Dickinson Immunocytometry Systems, San Jose, California, USA) were considered by the researcher.

Caspase 3 enzyme assay: As explained within the experiment of analysis of the cell cycle, the treatment of cells was carried out by using the same preparations for the duration of the same period (24 hrs). Later on, the cells were lysed, which was followed by the extraction and subjection of cells to caspase 3 content determination assay, by consuming a commercial kit. The entire procedure was performed according to the instructions provided by the manufacturers (USCN Life Science Inc., Wuhan, Hubei, China).

Statistical analysis: The presentation of data was performed using mean±SD. The IBM Statistical Package for Social Science (SPSS) statistics software (version 25) (SPSS Inc., Chicago, IL, USA) was utilized for carrying out statistical analysis. The means were compared by using the analysis of variance (ANOVA), which was then followed by Tukey's post hoc test. The statistical significance was indicated by $p<0.05$.

RESULTS

Preparation and characterization of TQ-TPGS NPs: Particle size results of the prepared TQ-ZN formulation showed an average size of (175±8.2 nm) as measured by Zetasizer Nano ZSP. TEM micrograph of the prepared TQ-ZN (Fig. 1) showed spherical nanospheres with comparative results with that obtained by the zetasizer.

***In vitro* release of TQ-ZN NPs formula:** The *in vitro* release profile of optimized TQ-ZN is shown in Fig. 2. The TQ-ZN NPs showed a burst release of TQ was observed. After 6 hrs, around 25% of TQ was released from NPs. At the end of 24 hrs, 80% of TQ released.

Determination of TQ-ZN NPs IC_{50} values: The data in Fig. 3 demonstrated the IC_{50} values acquired for the samples. TQ-ZN NPs had the least IC_{50} value, i.e., 2.5±1.2 µM, whereas TQ-raw had an IC_{50} value of 17.6±3.2 µM. Thus, when TQ was loaded in the NPs, there was a decline to about half of the value of IC_{50}.

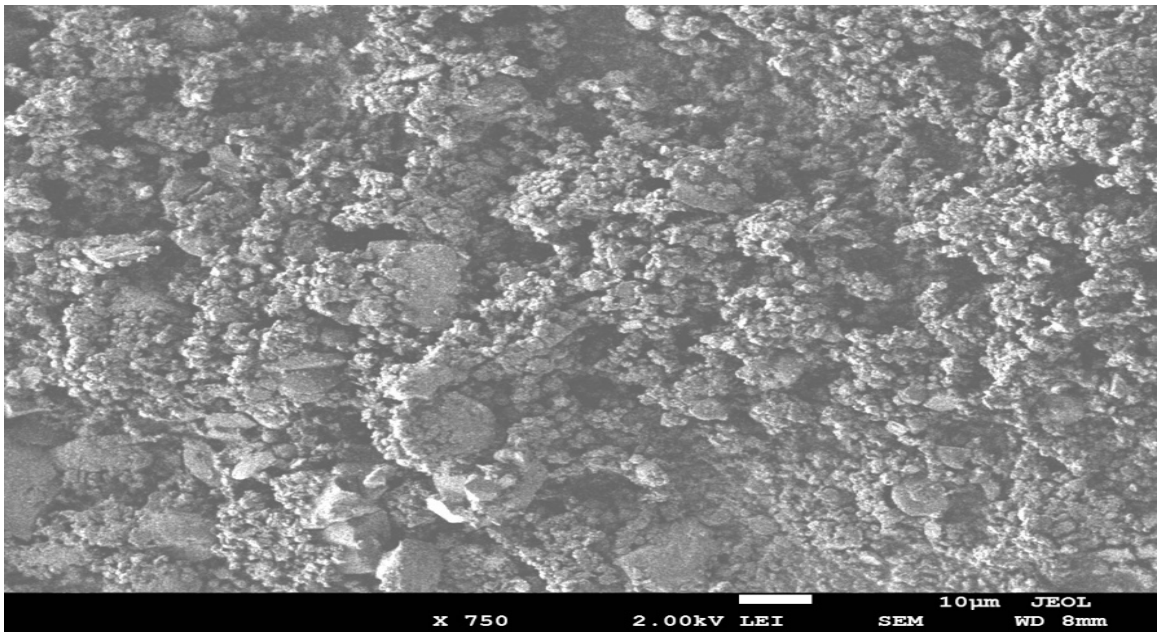

Fig. 1: Scanning electron microscope image of TQ-ZN NPs (×10,000)

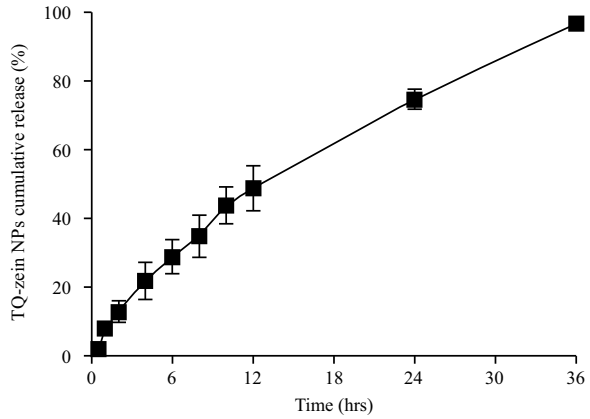

Fig. 2: *In vitro* release profile of TQ-ZN NPs in phosphate-buffered saline (PBS) buffer pH 7.4 at 37±0.5°C
Results are presented as mean±SD, n = 3

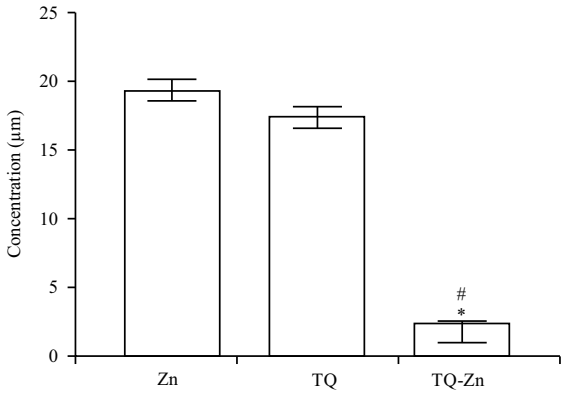

Fig. 3: IC_{50} of the ZN, TQ-raw, or TQ-ZN NPs in the MCF-7 cells
*Significantly different from control at p<0.05, #Significantly different from plain-M at p<0.05, $ significantly different from TQ-raw at p<0.05

Analysis of the cell cycle: The results of cell cycle analysis were presented in Fig. 4, demonstrating a substantial difference within the cell cycle. Observations revealed that the performance of TQ-ZN in all phases was according to expectations and there were no significant effects of plain-M on the G0-G1 phase. The cells percentage within the G_2-M phase demonstrated noticeable improvement in incubation with TQ-ZN. Thus, as compared to other samples, these effects were more noteworthy. The pre-G1 apoptosis also demonstrated a similar effect.

Annexin V staining: The analysis of apoptosis determination by flow cytometry was performed by using the Annexin V-FITC apoptosis detection kit. The data of Fig. 5 presented that in comparison with the other treatments, TQ-ZN exhibited higher and distinct early, late, as well as total cell apoptosis and cell death by necrosis.

Caspase-3 assay: TQ-ZN contributed to caspase-3 content's substantial enhancement (Fig. 6), resulting in approximately a two-fold increment, as compared to cells treated by TQ-raw. Moreover, caspase-3 content was induced by Plain-NPs, in comparison to the control value.

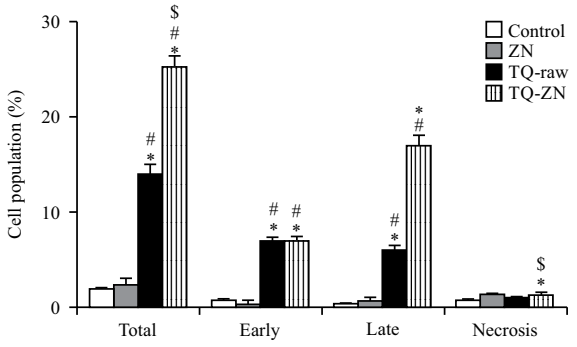

Fig. 4: Assessment of MCF-7 cell death using flow cytometric analysis after annexin V staining

*Significantly different from control at p<0.05, #Significantly different from plain-M at p<0.05, $significantly different from TQ-raw at p<0.05

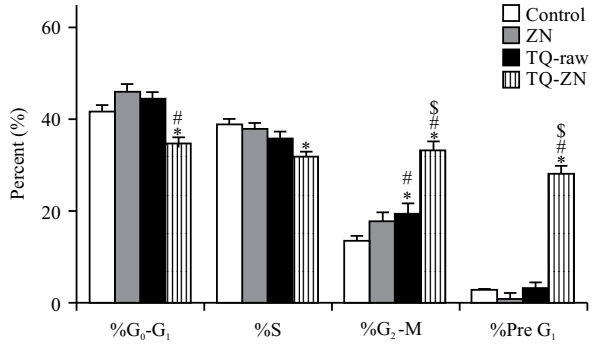

Fig. 5: Impact of ZN, TW-raw, TQ-ZN NPs treatments on the annexin-V FITC positive-staining of MCF-7 cells. N.B.: G_1, S, G_2 and M. The S represents cell cycle phases that gica an indicator for cell death via apoptosis

*Significantly different from control at p<0.05, #Significantly different from plain-M at p<0.05, $Significantly different from TQ-raw at p<0.05

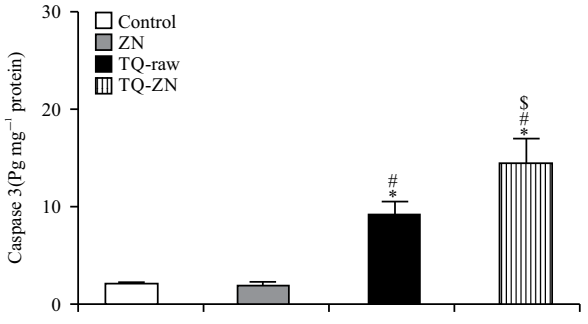

Fig. 6: Effect of TQ-ZN on caspase-3 content in MCF-7 cells

*Significantly different from control at p<0.05, #Significantly different from plain-M at p<0.05, $Significantly different from TQ-raw at p<0.05

DISCUSSION

In this study, the formulation of TQ loaded ZN NPs to evaluate the role of ZN as a drug carrier and sustain the release of TQ and enhance TQ cytotoxic activity against breast cancer cells. TQ-Zein NPs revealed spherical shaped NPs with *in vitro* TQ sustained release for over 36 hrs and enhanced cytotoxicity activity in MCF-7 cells when compared with either pure TQ or ZN.

The initial TQ release is related to the surface-bound release of TQ. The NPs showed sustained TQ release as a result of diffusion of TQ from NPs core through the hydrophobic ZN matrix[33]. The results of raw TQ against MCF-7 cells are per the results reported previously[47]. On the other hand, IC_{50} data agree with a previous report[17]. The reduction in the IC_{50} value of TQ loaded ZN NPs indicating that the nanocarrier system improved the activity of TQ. This finding is similar to the reported data of TQ in the human lung cancer line (MCF-7 cells)[35]. Our findings showed that TQ efficacy as a cytotoxic agent was augmented by loading in ZN NPs. This could be related to improved TQ's cellular permeability by the nanocarrier, modification of the TQ cellular uptake mechanism. Raw TQ is transported into cells by passive transport, while the TQ-ZN NPs transport mechanism is endocytosis. Besides, the encapsulation of drugs by ZN as hydrophobic nanospheres could improve cellular uptake across the cell membrane that leads to increased intracellular TQ concentration[48].

Apoptosis is a mechanism that regulates cell death at a genetic level, leads to the removal of harmed cells. The TQ-TQ-ZN NPs effect on G_2-M phases of the MCF-7 cell line indicated that TQ loaded ZN NPs formula augmented TQ efficacy. The improved MCF-7 cell percentage in the pre-G_1 cell cycle phase indicates apoptotic potential[39]. The apoptosis induction with the increased TQ efficiency for arresting at different cell cycle stages can be correlated to the capability of modulating the cellular components expressions, during the pathways of cell signaling, cell-cycle arrest and apoptosis. The evidence reported similar findings related to cancer cells[9].

Based on the findings and the previous outcomes of the analysis of the cell cycle, it can be stated that the increment in TQ's apoptotic potential is due to the arresting of different phases of the cell cycle. The present data is supported by the outcomes of previous reports and demonstrated that TQ can contribute to the arrest of colorectal cancer cells (HCT 116) within the G_2-M phase. Moreover, *in vitro*, TQ contributed to a G2/M phase cell cycle arrest in TFK1 as well as HuCCT-1 cells and decreased the expression of G2/M checkpoint protein

cyclin B1. Moreover, TQ also caused a significant increment in the percentage of the apoptotic cells in the pre-G phase[23,27]. The available evidence revealed that TQ blocks the cells in the G_0-G_1 phase[14,16]. Thus, in support of the previously published studies, it can be stated that apoptosis induction can be referred to as a mechanism of TQ's anti-proliferative properties[40]. Regarding annexin V, the current data acquire support from the previously published studies demonstrating that enhanced staining of melanoma cells with annexin V, after being challenged with TQ. Moreover, TQ-ZN NPs demonstrated a significant increment in the proportion of the MCF-7 cells with positive annexin staining. In the present research, the caspase-3 content was signi cantly enhanced by TQ-ZN NPs. Thus, along with the previous reports, the present outcomes indicated that TQ can enhance cellular caspase-3[34-39]. Previous researches have demonstrated that TQ-ZN NPs' enhanced effects on the cleaved content of caspase-3 in A543 cells[39]. The cleaved content caspase-3's elevation is considered as the latter cytosolic occurrence before apoptosis. Thus, the formulation of TQ in a nano-structured system improves the content of caspase-3. The advancement of activity of cleaved caspase-3 by the anti-tumor agents' nano-structured systems has also been previously reported[27]. Thus, the outcome also indicates the observed enhancement of caspase-3 content. Finally, this study confirms the efficiency of TQ in the suppression of breast cancer cells via induction of cancerous cell apoptosis especially by using ZN as a carrier. Clinical studies should be applied to confirm these findings.

CONCLUSION

The formulated TQ-ZN NPs were almost spherical. *In vitro* release of TQ from NPs was markedly delayed-release, predicting a better presentation to the tumor cells. TQ-ZN NPs significantly enhances their cytotoxic activities against MCF-7 cells. This is mediated, at least partly, by enhanced apoptosis as evidenced by cell cycle analysis, annexin V staining and determination of caspase 3 which improved cytotoxicity of TQ-ZN Nps.

SIGNIFICANCE STATEMENT

This study revealed the importance of ZN NPs as a novel system for improved delivery and augment the effect of TQ in cancer therapy. The results indicated the improved cytotoxic effects of TQ loaded ZN NPs when compared with raw TQ. This can be beneficial for the treatment of breast cancer with minimum side effects as TQ is approved as a safe drug. This study will shed light on researchers and oncologists to identify the importance of nanocarriers in cancer therapy.

ACKNOWLEDGMENT

This Project was funded by the Deanship of Scientific Research (DSR) at King Abdulaziz University, Jeddah, under grant no. (G-170-166-1441). The authors, therefore, acknowledge with thanks DSR for technical and financial support.

REFERENCES

1. Wu, M. and Y. Ding, 2018. Bioequivalence and pharmacokinetic profiles of abiraterone acetate 250-mg tablets in healthy Chinese subjects under fasted and fed condition: A four-way replicate crossover study by a RSABE approach. J. Bioequivalence Bioavailability, Vol. 10. 10.4172/0975-0851-c1-034.
2. Jung, Y.Y., J.H. Lee, D. Nam, A.S. Narula and O.A. Namjoshi *et al*., 2018. Anti-myeloma effects of icariin are mediated through the attenuation of JAK/STAT3-dependent signaling cascade. Front. Pharmacol., Vol. 9. 10.3389/fphar.2018.00531.
3. Khader, M. and P.M. Eckl, 2014. Thymoquinone: An emerging natural drug with a wide range of medical applications. Iran. J. Basic Med. Sci., 17: 950-957.
4. Ismail, A.F.H., F. Mohamed, L.M.M. Rosli, M.A.M. Shafri, M.S. Haris and A.B. Adina, 2016. Spectrophotometric determination of gentamicin loaded PLGA microparticles and method validation via ninhydrin-gentamicin complex as a rapid quantification approach. J. Applied Pharm. Sci., 6: 7-14.
5. Gali-Muhtasib, H., A. Roessner and R. Shneider-Stock, 2006. Thymoquinone: A promising anti-cancer drug from natural sources. Intl. J. Biochem. Cell Biol., 38: 1249-1253.
6. Schneider-Stock, R., I.H. Fakhoury, A.M. Zaki, C.O. El-Baba and H.U. Gali-Muhtasib, 2014. Thymoquinone: Fifty years of success in the battle against cancer models. Drug Discovery Today, 19: 18-30.
7. Shoieb, A.M., M. Elgayyar, P.S. Dudrick, K.L. Bell and P.K. Tithof, 2003. *In vitro* inhibition of growth and induction of apoptosis in cancer cell lines by thymoquinone. Int. J. Oncol., 22: 107-113.
8. Kalam, M.A., M. Raish, A. Ahmed, K.M. Alkharfy and K. Mohsin *et al*., 2017. Oral bioavailability enhancement and hepatoprotective effects of thymoquinone by self-nanoemulsifying drug delivery system. Mater. Sci. Eng. C, 76: 319-329.
9. Yin, Y.S., D.W. Chen, M.X. Qiao, Z. Lu and H.Y. Hu, 2006. Preparation and evaluation of lectin-conjugated PLGA nanoparticles for oral delivery of thymopentin. J. Controlled Release, 116: 337-345.

10. Bhattacharya, S., M. Ahir, P. Patra, S. Mukherjee and S. Ghosh *et al*., 2015. PEGylated-thymoquinone-nanoparticle mediated retardation of breast cancer cell migration by deregulation of cytoskeletal actin polymerization through miR-34a. Biomaterials, 51: 91-107.
11. Gali-Muhtasib, H.U., W.G. Abou Kheir, L.A. Kheir, N. Darwiche and P.A. Crooks, 2004. Molecular pathway for thymoquinone-induced cell-cycle arrest and apoptosis in neoplastic keratinocytes. Anticancer Drugs, 15: 389-399.
12. El-Najjar, N., M. Chatila, H. Moukadem, H. Vuorela and M. Ocker *et al*., 2010. Reactive oxygen species mediate thymoquinone-induced apoptosis and activate ERK and JNK signaling. Apoptosis, 15: 183-195.
13. Acharya, B.R., A. Chatterjee, A. Ganguli, S. Bhattacharya and G. Chakrabarti, 2014. Thymoquinone inhibits microtubule polymerization by tubulin binding and causes mitotic arrest following apoptosis in A549 cells. Biochimie, 97: 78-91.
14. Park, E.J., A.K. Chauhan, K.J. Min, D.C. Park and T.K. Kwon, 2016. Thymoquinone induces apoptosis through downregulation of c-FLIP and Bcl-2 in renal carcinoma caki cells. Oncol. Rep., 36: 2261-2267.
15. Ng, W.K., L.S. Yazan, L.H. Yap, W.A.G.W.N. Hafiza, C.W. How and R. Abdullah, 2015. Thymoquinone-loaded nanostructured lipid carrier exhibited cytotoxicity towards breast cancer cell lines (MDA-MB-231 and MCF-7) and cervical cancer cell lines (HeLa and SiHa). BioMed Res. Int., Vol. 2015. 10.1155/2015/263131.
16. Samarghandian, S., M. Azimi Nezhad and T. Farkhondeh, 2019. Thymoquinone induced antitumor and apoptosis in human lung adenocarcinoma cells. J. Cell Physiol., 234: 10421-10431.
17. Soni, P., J. Kaur and K. Tikoo, 2015. Dual drug-loaded paclitaxel–thymoquinone nanoparticles for effective breast cancer therapy. J. Nanopart. Res., Vol. 17. 10.1007/s11051-014-2821-4.
18. Rajput, S., N. Puvvada, B.N.P. Kumar, S. Sarkar and S. Konar *et al*., 2015. Overcoming Akt induced therapeutic resistance in breast cancer through siRNA and thymoquinone encapsulated multilamellar gold niosomes. Mol. Pharm., 12: 4214-4225.
19. Argos, P., K. Pedersen, M.D. Marks and B.A. Larkins, 1982. A structural model for maize zein proteins. J. Biol. Chem., 257: 9984-9990.
20. Bugs, M.R., L.A. Forato, R.K. Bortoleto-Bugs, H. Fischer, Y.P. Mascarenhas, R. Ward and L.A. Colnago, 2004. Spectroscopic characterization and structural modeling of prolamin from maize and pearl millet. Eur. Biophys. J., 33: 335-343.
21. Geraghty, D., M.A. Peifer, I. Rubenstein and J. Messing, 1981. The primary structure of a plant storage protein: Zein. Nucl. Acids Res., 9: 5163-5174.
22. Kasaai, M.R., 2018. Zein and zein -based nano-materials for food and nutrition applications: A review. Trends Food Sci. Technol., 79: 184-197.
23. Padua, G.W. and Q. Wang, 2009. Controlled Self-Organization of Zein Nanostructures for Encapsulation of Food Ingredients. In: ACS Symposium Series, Huang, Q., P. Given and M. Qian (Eds.)., ACS Publications, Washington, D.C., America pp: 143-156.
24. Corradini, E., P. Curti, A. Meniqueti, A. Martins, A. Rubira and E. Muniz, 2014. Recent advances in food-packing, pharmaceutical and biomedical applications of zein and zein-based materials. Int. J. Mol. Sci., 15: 22438-22470.
25. Zou, T., Z. Li, S.S. Percival, S. Bonard and L. Gu, 2012. Fabrication, characterization and cytotoxicity evaluation of cranberry procyanidins-zein nanoparticles. Food Hydrocolloids, 27: 293-300.
26. Ahmed, O.A.A., A. Zidan and M. Khayat, 2016. Mechanistic analysis of zein nanoparticles/PLGA triblock in situ forming implants for glimepiride. Int. J. Nanomed., 11: 543-555.
27. Penalva, R., C.J. González-Navarro, C. Gamazo, I. Esparza and J.M. Irache, 2017. Zein nanoparticles for oral delivery of quercetin: Pharmacokinetic studies and preventive anti-inflammatory effects in a mouse model of endotoxemia. Nanomed. Nanotechnol. Biol. Med., 13: 103-110.
28. Chen, H. and Q. Zhong, 2015. A novel method of preparing stable zein nanoparticle dispersions for encapsulation of peppermint oil. Food Hydrocolloids, 43: 593-602.
29. Bouman, J., P. Belton, P. Venema, E. van der Linden, R. de Vries and S. Qi, 2016. Controlled release from zein matrices: Interplay of drug hydrophobicity and pH. Pharm. Res., 33: 673-685.
30. Hu, K. and D.J. McClements, 2014. Fabrication of surfactant-stabilized zein nanoparticles: A pH modulated antisolvent precipitation method. Food Res. Int., 64: 329-335.
31. Mason, S.A., V.G. Welch and J. Neratko, 2018. Synthetic polymer contamination in bottled water. Front. Chem., Vol. 6. 10.3389/fchem.2018.00407.
32. Lai, L.F. and H.X. Guo, 2011. Preparation of new 5-fluorouracil-loaded zein nanoparticles for liver targeting. Int. J. Pharm., 404: 317-323.
33. Algandaby, M.M., M.M. Al-Sawahli, O.A.A. Ahmed, U.A. Fahmy and H.M. Abdallah *et al*., 2016. Curcumin-Zein nanospheres improve liver targeting and antifibrotic activity of curcumin in carbon tetrachloride-induced mice liver fibrosis. J. Biomed. Nanotechnol., 12: 1746-1757.
34. Zou, L., B. Zheng, R. Zhang, Z. Zhang and W. Liu *et al*., 2016. Enhancing the bioaccessibility of hydrophobic bioactive agents using mixed colloidal dispersions: Curcumin-loaded zein nanoparticles plus digestible lipid nanoparticles. Food Res. Int., 81: 74-82.

35. Dai, L., R. Li, Y. Wei, C. Sun, L. Mao and Y. Gao, 2018. Fabrication of zein and rhamnolipid complex nanoparticles to enhance the stability and *in vitro* release of curcumin. Food Hydrocolloids, 77: 617-628.
36. Ahmed, O.A.A., 2018. Development and single dose clinical pharmacokinetics investigation of novel zein assisted- alpha lipoic acid nanoencapsulation of vardenafil. Sci. Rep., Vol. 8. 10.1038/s41598-018-34235-8.
37. Baspinar, Y., M. Üstündas, O. Bayraktar and C. Sezgin, 2018. Curcumin and piperine loaded zein-chitosan nanoparticles: Development and *in vitro* characterisation. Saudi Pharm. J., 26: 323-334.
38. Ahmed, O.A.A., K.M. Hosny, M.M. Al-Sawahli and U.A. Fahmy, 2015. Optimization of caseinate-coated simvastatin-zein nanoparticles: Improved bioavailability and modified release characteristics. Drug Des. Dev. Ther., 9: 655-662.
39. Regier, M.C., J.D. Taylor, T. Borcyk, Y. Yang and A.K. Pannier, 2012. Fabrication and characterization of DNA-loaded zein nanospheres. J. Nanobiotechnol., Vol. 10. 10.1186/1477-3155-10-44.
40. El-Say, K.M., O.A.A. Ahmed, A.I. Mohamed, M.K. Safo and A.S.M. Omar, 2019. Zein-alpha lipoic acid-loaded nanoparticles to enhance the oral bioavailability of dapoxetine: optimization and clinical pharmacokinetic evaluation. Int. J. Nanomed., 14: 7461-7473.
41. Díaz-Gómez, J., M. Ortíz-Martínez, O. Aguilar, S. García-Lara and F. Castorena-Torres, 2018. Antioxidant activity of zein hydrolysates from zea species and their cytotoxic effects in a hepatic cell culture. Molecules, Vol. 23. 10.3390/molecules 23020312.
42. Alhakamy, N.A., O.A.A. Ahmed, H.M. Aldawsari, M.Y. Alfaifi, B.G. Eid, A.B. Abdel-Naim and U.A. Fahmy, 2019. Encapsulation of lovastatin in zein nanoparticles exhibits enhanced apoptotic activity in HepG2 cells. Int. J. Mol. Sci., Vol. 20. 10.3390/ijms20225788.
43. Kurakula, M., O.A.A. Ahmed, U.A. Fahmy and T.A. Ahmed, 2016. Solid lipid nanoparticles for transdermal delivery of avanafil: Optimization, formulation, *in-vitro* and *ex-vivo* studies. J. Liposome Res., 26: 288-296.
44. Safwat, S., R.A. Ishak, R.M. Hathout and N.D. Mortada, 2017. Nanostructured lipid carriers loaded with simvastatin: Effect of PEG/glycerides on characterization, stability, cellular uptake efficiency and *in vitro* cytotoxicity. Drug Dev. Ind. Pharm., 43: 1112-1125.
45. Ahmed, O.A., U.A. Fahmy, A.S. Al-Ghamdi, B.M. Aljaeid and H. Aldawsari *et al*., 2017. Finasteride-loaded biodegradable nanoparticles: Near-infrared quantification of plasma and prostate levels. J. Bioact. Compatible Polym., 32: 557-567.
46. Fahmy, U.A., 2016. Quantification of simvastatin in mice plasma by near-infrared and chemometric analysis of spectral data. Drug Des. Dev. Ther., 10: 2507-2513.
47. Shrestha, N., S. Khan, Y.R. Neupane, S. Dang and S. Md *et al*., 2020. Tailoring midazolam-loaded chitosan nanoparticulate formulation for enhanced brain delivery via intranasal route. Polymers, Vol. 12. 10.3390/polym12112589.
48. Yeganeh, B., E. Wiechec, S.R. Ande, P. Sharma and A.R. Moghadam *et al*., 2014. Targeting the mevalonate cascade as a new therapeutic approach in heart disease, cancer and pulmonary disease. Pharmacol. Therapeut., 143: 87-110.
49. Sekine, Y., H. Nakayama, Y. Miyazawa, H. Kato and Y. Furuya *et al*., 2018. Simvastatin in combination with meclofenamic acid inhibits the proliferation and migration of human prostate cancer PC-3 cells via an AKR1C3 mechanism. Oncol. Lett., 15: 3167-3172.